Heavy Quark Transport Is Non-Gaussian beyond Leading Logarithm

Jean F. Du Plessis[1,2,*] and Bruno Scheihing-Hitschfeld[2,†]

[1]Center for Theoretical Physics—A Leinweber Institute, Massachusetts Institute of Technology, Cambridge, Massachusetts 02139, USA
[2]Kavli Institute for Theoretical Physics, University of California, Santa Barbara, California 93106, USA

(Received 12 May 2026; revised 8 September 2026; accepted 22 September 2026; published 5 November 2026)

We find that heavy quark transport beyond leading logarithm at weak coupling is intrinsically non-Gaussian: the longitudinal momentum transfer distribution has *asymmetric exponential tails* that are crucial for equilibration dynamics. We show this by computing the leading-order momentum transfer kernel for relativistic heavy quarks in weakly coupled non-Abelian plasmas, matching perturbative momentum transfer on the thermal scale to hard-thermal-loop-resummed soft physics. This is the same structure previously found in strongly coupled holographic plasmas, showing that it is not peculiar to weak or strong coupling, conformality, or supersymmetry. We therefore expect that this is a robust feature that physical quark-gluon plasma should also exhibit.

DOI: 10.1103/7fd5-1kq5

Heavy quarks (HQs) provide a particularly valuable probe of the quark-gluon plasma (QGP) produced in ultra-relativistic heavy-ion collisions (HICs). Because they are long-lived on quantum chromodynamics (QCD) time-scales and interact directly with the thermal medium, their propagation offers a sensitive window into how colored probes exchange energy and momentum with QGP constituents. This separation of scales makes heavy quarks natural candidates for a Brownian-motion-like description, and motivated early Langevin and Fokker-Planck treatments of heavy-flavor transport [1–4] shortly after data became available. Together with Boltzmann transport approaches, they constitute the state of the art of heavy quark transport [5–10]. The nonperturbative determination of the HQ diffusion coefficient [1,11], the essential QCD input for a Langevin description, is by now mature in the $v \to 0$ limit using lattice QCD methods [12–17] in tandem with perturbative calculations [18–22], providing an increasingly sharp first-principles input for phenomenological comparisons to heavy-ion collision data.

However, challenges still remain. It has long been understood [1] that, for a heavy quark moving through a weakly coupled plasma, the Einstein relation $\kappa_L = 2MT\gamma\eta_D$ between the drag η_D and longitudinal diffusion coefficients κ_L—the necessary condition for kinetic equilibration to take place in a (Gaussian) Langevin description—is violated at nonzero velocity once one goes beyond leading logarithmic accuracy. The Einstein relation is also violated in strongly coupled $\mathcal{N} = 4$ supersymmetric Yang-Mills (SYM) theory [23–26]. In a purely Langevin or Fokker-Planck description this is a serious obstruction to connecting first-principles calculations with phenomenological descriptions [27]. Until now, this issue had not been resolved in perturbative QCD. Furthermore, the problem is not merely formal. Boltzmann transport studies have shown that non-Gaussian momentum transfer dynamics can modify heavy-flavor observables and the transport coefficients extracted from them [28,29], which may be relevant to the tension between phenomenological extractions and lattice QCD determinations of heavy quark transport coefficients [30].

Recent work has clarified the conceptual resolution of this issue. When retaining the full momentum transfer statistics of the process, heavy quark evolution is governed not by a Fokker-Planck equation but by a Kolmogorov equation, and equilibration is controlled by a universal non-Gaussian condition on the corresponding kernel [31]. In strongly coupled $\mathcal{N} = 4$ SYM, the full leading order kernel was shown to satisfy this generalized equilibration condition and to exhibit a distinctive non-Gaussian longitudinal momentum transfer distribution [32]. This raises a natural question: is the same non-Gaussian structure present for heavy quarks in weakly coupled gauge theory plasmas?

In this Letter we answer that question in the affirmative. We find that heavy quark transport at weak coupling beyond leading logarithm exhibits manifest non-Gaussian structure: the longitudinal momentum transfer distribution has a Gaussian core and asymmetric exponential tails. The tails are essential for equilibration in light of the violation of the Einstein relation [31], meaning that HQ transport is intrinsically non-Gaussian. The Gaussian core follows as a natural consequence of the central limit

*Contact author: jeandp@mit.edu
†Contact author: bscheihi@kitp.ucsb.edu

Published by the American Physical Society under the terms of the Creative Commons Attribution 4.0 International license. Further distribution of this work must maintain attribution to the author(s) and the published article's title, journal citation, and DOI. Funded by SCOAP³.

theorem. On the other hand, the exponential tails are a new and surprising result. In fact, this structure is also present in the strongly coupled calculation of [32]—a fact that has remained underappreciated so far. With weakly coupled QCD and both weakly *and* strongly coupled $\mathcal{N}=4$ SYM exhibiting this same structure, this indicates that Gaussian core and exponential tail momentum transfer is not peculiar to weak or strong coupling, conformality, or supersymmetry, but is instead likely to be a robust feature of realistic QGP. To establish this result, we consistently match the ultraviolet (UV) perturbative contribution to the infrared hard thermal loop (HTL) sector, isolate the strict fixed-order kernel, and determine the longitudinal momentum transfer distribution at all momenta via a Legendre transform. The full matched kernel reproduces the known leading-log results for the drag and momentum diffusion coefficients, as well as the known leading-order diffusion coefficient at $\mathbf{v}=\mathbf{0}$, thereby recovering the appropriate Gaussian limits. It also satisfies the generalized equilibration condition of Ref. [31], providing a nontrivial consistency check on the resulting non-Gaussian dynamics.

Setup—We work in the large mass limit, neglecting all mass-dependent effects at the level of transition probabilities. Formally, we work at leading order in the heavy quark effective theory (HQET) expansion of the QCD Lagrangian [33], neglecting $1/M$ corrections. In this regime the momentum transfer distribution of the heavy quark to the medium over a time Δt is determined by the Fourier transform of a Wilson loop,

$$P(\mathbf{k};\mathbf{v})=\int\frac{d^3\mathbf{L}}{(2\pi)^3}e^{-i\mathbf{k}\cdot\mathbf{L}}\langle W_{\mathbf{v}}\rangle(\mathbf{L};\Delta t), \tag{1}$$

which can be formulated on the Schwinger-Keldysh contour [31,32]. In the late-time limit, the separation of scales $M\gg T$ implies that heavy quarks undergo Markovian dynamics due to the shortness of the medium equilibration timescale $\sim 1/T$ relative to the time needed to appreciably modify the velocity of the heavy quark. For such timescales $\Delta t\gg 1/T$, we have

$$\langle W_{\mathbf{v}}\rangle(\mathbf{L};\Delta t)=\exp\left[-(\Delta t)T\,S(\mathbf{L};\mathbf{v})+\cdots\right], \tag{2}$$

which defines the momentum transfer kernel $S(\mathbf{L};\mathbf{v})$.

At weak coupling, a consistent leading-order result requires matching perturbative "hard" momentum transfer ($p\sim T$) (following from finite temperature Feynman diagrams [34–37]) to HTL "soft" physics [38–41] ($p\sim gT$) while subtracting their overlap,

$$(\text{Result})=(\text{Pert.})+(\text{HTL})-(\text{HTL, unresummed}). \tag{3}$$

This procedure has been used to calculate the HQ diffusion coefficient [20]. By definition, subextensive contributions in Δt do not contribute to S, and by unitarity of the Wilson lines that make up the loop we have

$$S(\mathbf{L}=\mathbf{0};\mathbf{v})=0. \tag{4}$$

Consequently, the calculation reduces to extracting only those contributions that are simultaneously $\mathbf{L}$ dependent and extensive in Δt. Denoting $\int_{\mathbf{p}}\equiv\int d^3\mathbf{p}/(2\pi)^3$, the matched weak-coupling kernel may then be written as

$$S(\mathbf{L};\mathbf{v})=-\frac{g^2C_F}{T}\int_{\mathbf{p}}\frac{e^{i\mathbf{p}\cdot\mathbf{L}}-1}{1-e^{-\mathbf{p}\cdot\mathbf{v}/T}}\{g^2\mathcal{I}_{\text{Hard}}(\mathbf{p},\mathbf{v};T,N_c,N_X,N_f) +\mathcal{I}_{\text{Soft}}(\mathbf{p},\mathbf{v};m_D^2)-\mathcal{I}_{\text{Match}}(\mathbf{p},\mathbf{v};m_D^2)\}, \tag{5}$$

where we give the full form of each term in the End Matter. We also note the appearance of the Debye mass $m_D^2=g^2T^2[N_c/3+N_cN_X/6+T_FN_f/3]$ in the soft and matching integrands [42]. Its structure immediately implies

$$S(\mathbf{L};\mathbf{v})=S(i\mathbf{v}/T-\mathbf{L};\mathbf{v}), \tag{6}$$

which is precisely the generalized equilibration condition derived in Ref. [31]. Its small velocity expansion recovers the Einstein relation, whereby a Gaussian truncation becomes consistent with equilibration as $v\to 0$, although higher (even) cumulants generically remain nonzero at $v=0$. Einstein-relation violation is therefore a finite velocity effect, but non-Gaussianity is present at all velocities. For present purposes, however, the central role of Eq. (5) is to define the longitudinal momentum-transfer distribution whose shape we analyze below in a controlled weak-coupling expansion. The symmetry in Eq. (6) then provides a nontrivial consistency check on that construction. Because this symmetry is a structural property of the integrand in Eq. (5), independent of the specific forms of $\mathcal{I}_{\text{Hard}}$, $\mathcal{I}_{\text{Soft}}$, and $\mathcal{I}_{\text{Match}}$, the equilibration condition holds order by order in perturbation theory.

Fixed-order longitudinal kernel—To determine the shape of the weak-coupling momentum transfer distribution beyond leading logarithm, we must first isolate the strict fixed-order kernel. The matched kernel in Eq. (5) is correct through $\mathcal{O}(g^4)$, but it contains contamination from $\mathcal{O}(g^6)$ and higher terms generated by the HTL resummation.

This contamination becomes especially problematic when one attempts to extract information about the distribution from derivatives of the kernel at $\mathbf{L}=0$. The relevant quantities are the cumulants of the momentum transfer probability per unit time and temperature,

$$M_{i_1\ldots i_n}(\mathbf{v})=-\left.\frac{\partial^n S(\mathbf{L};\mathbf{v})}{\partial(iL_{i_1})\cdots\partial(iL_{i_n})}\right|_{\mathbf{L}=0}, \tag{7}$$

which characterize the statistical properties of $P(\mathbf{k};\mathbf{v})$, including quantities of high phenomenological interest such as the drag coefficient η_D encoded in M_i and the momentum broadening coefficients κ_T, κ_L encoded in M_{ij}. However, the cumulants in Eq. (7) become UV divergent for $n \geq 3$ due to the HTL contributions in Eq. (5). This obstructs the determination of the fixed-order kernel, and is also clearly unphysical. This is because for $|\mathbf{p}| \gg gT$ one has [43]

$$\mathcal{I}_{\rm Soft}(\mathbf{p},\mathbf{v};m_D^2) - \mathcal{I}_{\rm Match}(\mathbf{p},\mathbf{v};m_D^2) = \mathcal{O}\left(\frac{m_D^4}{|\mathbf{p}|^6}\right), \quad (8)$$

which, together with the overall g^2 prefactor in (5), is a strictly higher order contribution than the g^4 terms we are aiming to determine, and nonetheless yields an infinite contribution to the cumulants because of the aforementioned UV divergence.

A resolution to this problem can be achieved by inserting Heaviside step functions to separate the contributions in each regime (reminiscent of the original methods by Braaten and Thoma [44,45]). Concretely, writing

$$S(\mathbf{L};\mathbf{v}) = -\frac{g^2 C_F}{T}\int_{\mathbf{p}} \frac{e^{i\mathbf{p}\cdot\mathbf{L}}-1}{1-e^{-\mathbf{p}\cdot\mathbf{v}/T}}[\theta(|\mathbf{p}|-T) + \theta(T-|\mathbf{p}|)]\{g^2\mathcal{I}_{\rm Hard} + \mathcal{I}_{\rm Soft} - \mathcal{I}_{\rm Match}\}, \quad (9)$$

we may simply omit the HTL pieces for $|\mathbf{p}| > T$, since $\mathcal{I}_{\rm Soft} - \mathcal{I}_{\rm Match} = \mathcal{O}(m_D^4/|\mathbf{p}|^6)$. At this stage the result is manifestly fixed order except for the HTL-resummed contribution for $|\mathbf{p}| < T$.

In this (soft) region the $g \to 0$ limit and the momentum integral do not commute, so one must first perform the radial integral exactly and only then expand in $m_D/T \propto g$ in order to correctly determine the logarithmically enhanced $g^4\ln(1/g)$ terms. The result is

$$\begin{aligned} S_{\rm FO}(\mathbf{L};\mathbf{v}) = {}& \frac{g^2 C_F m_D^2}{4\pi}\ln\left(\frac{m_D}{T}\right)\left[\frac{(v^2-1)\operatorname{arctanh}(v)+v}{2v^3} iL_\parallel\left(iL_\parallel+\frac{v}{T}\right) + \frac{3v^3+(1-v^2)^2\operatorname{arctanh}(v)-v}{4v^3}(iL_\perp)^2\right] \\ & + \frac{g^2 C_F m_D^2}{4\pi}\int_0^1 d\mu\left[\mu^2 iL_\parallel\left(iL_\parallel+\frac{v}{T}\right)+\frac{1-\mu^2}{2}(iL_\perp)^2\right]\left[\Phi(a_E,b_E)+\frac{v^2(1-\mu^2)}{2(1-v^2\mu^2)}\Phi(a_T,b_T)\right] \\ & - \frac{g^2 C_F}{T}\int_{\mathbf{p}}\left\{g^2\frac{e^{i\mathbf{p}\cdot\mathbf{L}}-1}{1-e^{-\mathbf{p}\cdot\mathbf{v}/T}}\mathcal{I}_{\rm Hard} - \theta(T-|\mathbf{p}|)(\mathbf{p}\cdot i\mathbf{L})\left[\mathbf{p}\cdot\left(i\mathbf{L}+\frac{\mathbf{v}}{T}\right)\right]\frac{T}{2\mathbf{p}\cdot\mathbf{v}}\mathcal{I}_{\rm Match}\right\}, \end{aligned} \quad (10)$$

where

$$\Phi(a,b) \equiv \frac{1}{4}\ln(a^2+b^2) + \frac{a}{2b}\arctan\left(\frac{b}{a}\right), \quad (11)$$

and the functions $a_{E,T}$ and $b_{E,T}$ are defined in terms of $\eta = \mu v$ as

$$a_E \equiv 1 - \frac{\eta}{2}\ln\left(\frac{1+\eta}{1-\eta}\right), \qquad b_E \equiv \frac{\pi}{2}\eta, \quad (12)$$

$$a_T \equiv \frac{1}{2}\left[\frac{\eta^2}{1-\eta^2} + \frac{\eta}{2}\ln\left(\frac{1+\eta}{1-\eta}\right)\right], \qquad b_T \equiv \frac{\pi}{4}\eta. \quad (13)$$

Equation (10) is the complete fixed-order (denoted by the subscript "FO") kernel at order g^4. Its structure cleanly separates two physically distinct pieces. The first line of Eq. (10) contains the logarithmically enhanced piece [46], which we could also have obtained by directly translating the results of [1] for the transport coefficients η_D, κ_T, κ_L into our notation, and thus serves as a cross-check of our result. The last two lines contain the remaining fixed-order contribution, determined by the perturbative piece $\mathcal{I}_{\rm Hard}$ and the remaining g^4 terms coming from the HTL-resummed result and the matching. In particular, the last line generates arbitrarily high-order cumulants, all of which are finite. This can be seen by examining the exponential suppression of $\mathcal{I}_{\rm Hard}(\mathbf{p},\mathbf{v})$ at large $\mathbf{p}$ by statistical factors (see End Matter).

We have explicitly verified that replacing the separation scale T by any $\Lambda \sim T$ leaves the fixed-order kernel $S_{\rm FO}$ invariant. As an additional cross-check, we have verified that the second moment of the kernel at $\mathbf{v} = \mathbf{0}$ reproduces the known diffusion coefficient [1,20] exactly at order g^4. We discuss both in the End Matter; further derivations are provided in Supplemental Material [47].

Momentum transfer probability—To examine the physical implications of the fixed-order kernel, we proceed along the lines of [31] to calculate the momentum transfer probability in the late-time limit. For the equilibration dynamics of an isotropic distribution function, only the longitudinal projection contributes. We therefore start by introducing the longitudinal evolution kernel

$$K(x,v) \equiv S_{\rm FO}(\mathbf{L} = -ix\hat{\mathbf{v}};\mathbf{v} = v\hat{\mathbf{v}}) = -\sum_{n=1}^{\infty}\frac{\mathfrak{M}_n(v)}{n!}x^n, \quad (14)$$

where $\mathfrak{M}_n(v) \equiv \hat{\mathbf{v}}_{i_1}\cdots\hat{\mathbf{v}}_{i_n}M^{\rm FO}_{i_1\ldots i_n}$ are the projected (fixed order) cumulants per unit time of the momentum change

probability distribution obtained from the Taylor series of S_{FO} as in Eq. (7).

Inside the interval $-v/T < x < 0$, $K(x,v)$ is directly evaluated from the integral representation in Eq. (10). Outside this region, because all of its derivatives are finite and calculable, for $x > 0$ we determine it using the Taylor expansion around $x = 0$, and with the corresponding expansion around $x = -v/T$ implied by Eq. (6) for $x < -v/T$. The agreement of these expansions with the integral representation in their common domain provides a nontrivial check that the analytic continuation is under control.

In the Markovian limit, following [31], the longitudinal momentum transfer probability takes the form

$$P(k_L; v) = \exp\left(-tT\tilde{S}(C_L; v) + \cdots\right), \tag{15}$$

where $C_L = \mathbf{k}\cdot\hat{\mathbf{v}}/(tT)$ is the longitudinal momentum transfer rate, the dots "…" stand for nonextensive terms in t, and $\tilde{S}$ is the Legendre transform of the evolution kernel $K(x,v)$,

$$\tilde{S}(C_L; v) = \left[K(x,v) - x\,\frac{\partial K}{\partial x}\right]_{x=x(C_L)}, \tag{16}$$

where $x(C_L)$ is determined by the implicit relation

$$C_L = -\frac{\partial K}{\partial x}. \tag{17}$$

In this way, the cumulants $\mathfrak{M}_n$ not only characterize the longitudinal momentum transfer probability distribution, they explicitly determine it. Nonzero cumulants for $n \geq 3$ imply a non-Gaussian momentum transfer probability, because the resulting $\tilde{S}$ is manifestly not a quadratic function of C_L.

It is thus worth examining what structural properties are present in K beyond its symmetries. One such property that our calculation gives us access to, which, to our knowledge, has not received much attention in the literature, is the large n behavior of the longitudinal cumulants, which determines when the series (14) converges. In fact, at $v = 0$ the moments can be computed in closed form (see End Matter). The even cumulants scale as

$$\mathfrak{M}_n(0) \sim (2T)^n \frac{n!}{n^2}, \qquad n \to \infty, \qquad n \text{ even}, \tag{18}$$

giving a radius of convergence $R(v=0) = 1/(2T)$ for the series that determines K in Eq. (14). Similarly, in the ultrarelativistic limit $\gamma \gg 1$, the radius of convergence becomes $R(v) \sim 1/(4\gamma^2 T)$ [48]. $R(v)$ contains dynamical information about the microscopic nature of the medium: Applying the same characterization to the known strongly coupled $\mathcal{N} = 4$ SYM kernel [32], we obtain $R(v) \sim 1/(r_0\gamma^{\frac{3}{2}}T)$—featuring a different exponent for γ, with $r_0 \approx 1.7972$—sketched in the End Matter. Note that, both in the weak and strong coupling expansions, the leading contribution to $R(v)$ is independent of the coupling; coupling dependence only appears at subleading order in either expansion.

Furthermore, in both weakly coupled gauge plasmas and this strongly coupled theory, all of the cumulants are positive, and therefore K exhibits singularities at the edges of its domain of analyticity outside the interval $-v/T < x < 0$. Through Eq. (17), these edges map to $C_L \to \pm\infty$ due to the rapid growth of $\mathfrak{M}_n$ with n in all of these theories, and because the inverse Legendre transform gives $x = \partial\tilde{S}/\partial C_L$, the momentum transfer probability has exponential tails at large $|C_L|$, with its steepness in either direction set by the radius of convergence $R(v)$ of the kernel K and the asymmetry required by the universal equilibration condition [31]. Explicitly,

$$P(k_L) \propto e^{-R(v)k_L} \quad \text{as } k_L \to \infty, \tag{19}$$

$$P(k_L) \propto e^{+[R(v)+v/T]k_L} \quad \text{as } k_L \to -\infty. \tag{20}$$

This physical feature of the momentum transfer probability seems to be robust across all couplings (manifest in Fig. 1), directly connected to K having a finite, nonzero radius of convergence. Thus, the radius of convergence $R(v)$ of the Taylor expansion of $K(x,v)$ about $x = 0$ is also exactly the exponential decay rate of the positive large k_L tail. We therefore refer to this quantity as the *tail exponent*. The asymptotic negative-k_L decay rate is $R(v) + (v/T)$, fixed by the generalized equilibration condition.

As one might expect, the main driver of the exponential tails is the hard physics of the medium (in the HTL sense, i.e., $|\mathbf{p}| \sim T$; *not* in the HQET $|\mathbf{k}| \sim M$ sense), manifest in the fact that the high order cumulants are set by the perturbative contribution, and not the soft physics ($|\mathbf{p}| \sim gT$) described by HTL resummation. Looking at the structure of the calculation, it should remain true at any order in perturbation theory that the large n scaling of the cumulants, and therefore the radius of convergence, are solely influenced by the hard physics contributions. Furthermore, in an asymptotically free gauge theory, if the coupling runs with the momentum transfer, the tails of the momentum transfer should asymptotically be given by the leading order hard piece we have computed here.

To compare the shape of the longitudinal momentum transfer distribution (15) across velocities, couplings and theories, we normalize the logarithm of said distribution using its first two longitudinal cumulants and plot $(\mathfrak{M}_2/\mathfrak{M}_1^2)\tilde{S}(C_L; v)$ against $C_L/\mathfrak{M}_1$ in Fig. 1. With this normalization, the overall drag and width are scaled out, and any purely Gaussian process collapses onto a universal parabola, shown by the black dotted curve. Deviations from

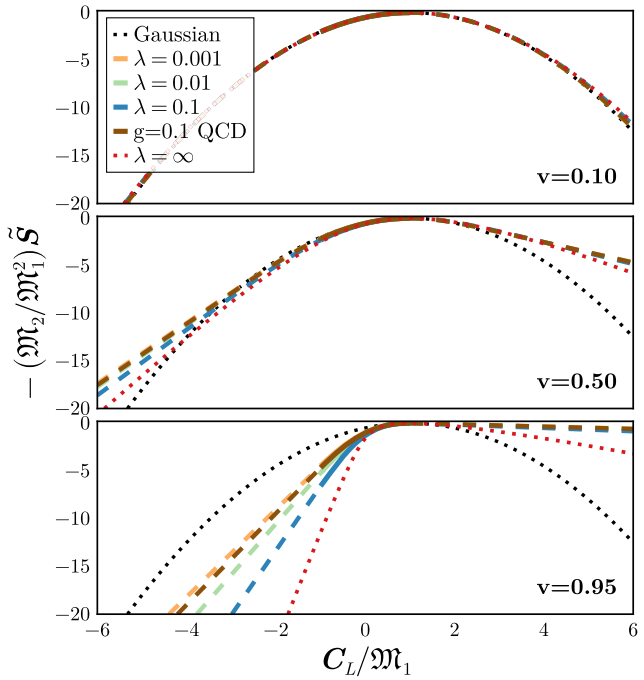


FIG. 1. Normalized log-probability density for longitudinal momentum transfer, shown as $(\mathfrak{M}_2/\mathfrak{M}_1^2)\tilde{S}(C_L; v)$ versus $C_L/\mathfrak{M}_1$ for $v = 0.10$, 0.50, and 0.95. Rescaling by the first two longitudinal cumulants removes the overall drag and width, so that any purely Gaussian process collapses onto the universal parabola shown by the black dotted curve; deviations from that parabola therefore isolate genuine non-Gaussian shape. Colored curves show the weak-coupling fixed-order result for $\mathcal{N} = 4$ SYM with $\lambda = g^2 N_c = 10^{-3}, 10^{-2}, 10^{-1}$ together with the weak-coupling massless $N_f = 3$ QCD result. Solid segments are obtained directly from the integral representation of Eq. (10) inside the interval $-v/T < x < 0$, while dashed segments are obtained by analytic continuation using the moments in Eq. (14). The red dotted curve is the strong-coupling $\mathcal{N} = 4$ SYM result of Ref. [32]. The figure shows that, once the Gaussian scale set by $\mathfrak{M}_1$ and $\mathfrak{M}_2$ is removed, weakly coupled $\mathcal{N} = 4$ SYM, strongly coupled $\mathcal{N} = 4$ SYM, and weakly coupled QCD all exhibit the same qualitative non-Gaussian structure.

that benchmark therefore isolate genuine non-Gaussian structure.

At low velocity, $v = 0.10$, the weak-coupling result remains close to the Gaussian benchmark in the range plotted. By $v = 0.50$, however, the distribution is already visibly skewed and non-Gaussian, and by $v = 0.95$ the deviation is pronounced on both sides of the extremum. Over the range $\lambda = 10^{-3} - 10^{-1}$ the normalized weakly coupled $\mathcal{N} = 4$ curves [49] have little spread, and the weak-coupling massless $N_f = 3$ QCD curve has the same qualitative shape. The strong-coupling $\mathcal{N} = 4$ SYM result of Ref. [32], shown as the red dotted curve, exhibits the same qualitative asymmetric non-Gaussian profile. Contrary to what Fig. 1 might suggest, we remark that as $tT \to \infty$ the bulk of the distribution is asymptotically approximated by a Gaussian distribution for any fixed v, as required by the central limit theorem. The tails—the feature that this figure is designed to highlight—characterize the rare events away from the (Gaussian) core of the distribution that become suppressed in the late time limit, but still retain a nonzero probability of occurrence. That being said, regardless of their small probability, the asymmetry of the exponential tails is in fact essential for heavy quark equilibration [31], which is evident in the fact that the Gaussian core *does not* satisfy the Einstein relation. Furthermore, for a realistic heavy quark with large but finite mass traversing the medium for a finite time, the asymptotic central limit theorem regime can never be fully reached: individual large kicks—precisely those described by the exponential tails—can appreciably change the quark's velocity $v \to v'$, forcing subsequent samplings to be from $P(k_L; v')$, which is not well-described by the original $P(k_L; v)$. Therefore, the tails carry non-negligible dynamical importance beyond their role in ensuring equilibration.

The agreement between weak and strong coupling in $\mathcal{N} = 4$ SYM that we see in Fig. 1, together with the same qualitative weak-coupling structure in QCD, suggests that Gaussian core and exponential tail momentum transfer is not peculiar to weak or strong coupling, conformality, or supersymmetry, but rather a robust feature that realistic QGP should also exhibit, with its *independent* Gaussian characteristics $\eta_D(v)$, $\kappa_L(v)$, and the tail exponent $R(v)$ as the primary properties of the dynamics.

Outlook—We have shown that the longitudinal momentum transfer distribution of a relativistic heavy quark in generic weakly coupled gauge theory plasmas has a Gaussian core and exponential tails, and that, in particular, weakly coupled QCD exhibits this behavior. This is the same qualitative structure previously found in strongly coupled $\mathcal{N} = 4$ SYM theory [32]. This indicates that these features might be generic across many gauge theory plasmas, regardless of their coupling strength or their matter content. In particular, neither conformality nor supersymmetry seem to play a significant role.

Isolating the strict fixed-order kernel was essential to making this structure calculable at weak coupling. Dissecting the two types of contributions to our result—distinguished by whether there is a logarithmic $\ln(1/g)$ enhancement—we find that only the Gaussian characteristics of the momentum transfer probability contain logarithmically enhanced terms. Accordingly, the log-enhanced terms satisfy the Einstein relation, as had long been known [1]. At finite velocity, however, the remaining fixed-order contributions control the shape of the distribution and invalidate a purely Gaussian truncation, as the universal equilibration condition [31] is only satisfied through a detailed balance of all of the cumulants. A Gaussian description is therefore not consistent with first-principles calculations for generic relativistic heavy-quark transport.

These results have direct implications for heavy-flavor phenomenology. Since non-Gaussian momentum transfer can modify heavy-flavor observables and the transport coefficients extracted from them [28–30], phenomenological descriptions based purely on Gaussian or Langevin truncations are not microscopically justified by default. Our calculation therefore motivates revisiting heavy-quark transport in the QGP with non-Gaussian kernels if one aims to extract transport coefficients that can be meaningfully compared to lattice determinations. A more realistic, *non-Gaussian* description may be organized in terms of $\eta_D(v)$, $\kappa_L(v)$, and a single additional parameter $R(v)$, the tail exponent, characterizing the distribution of (rare) large momentum kicks, which sets the slopes of the asymmetric exponential tails. Whether such a description can consistently account for heavy-flavor observables as the Pb-Pb program becomes increasingly precise in Run 3 and, in the longer term, with the proposed ALICE 3 detector upgrade [54], while also accommodating the complementary system-size constraints that should emerge from the recently collected O-O and Ne-Ne data, should provide a sharp test.

Acknowledgments—We gratefully acknowledge helpful conversations with Dani Pablos, Krishna Rajagopal, Rachel Steinhorst, Eamonn Weitz, Urs Wiedemann, and Xiaojun Yao. Research supported in part by the U.S. Department of Energy, Office of Science, Office of Nuclear Physics under grant Contract No. DE-SC0011090, by Grant No. NSF PHY-2309135 to the Kavli Institute for Theoretical Physics (KITP), and by Grant No. 994312 from the Simons Foundation. This research has benefited from the Mitchel Postdoctoral Scholar Career Development Fund at KITP.

Data availability—There are no publicly available research data or software supporting this manuscript. Requests for further information or data should be sent to the authors.

[1] G. D. Moore and D. Teaney, Phys. Rev. C **71**, 064904 (2005).
[2] H. van Hees and R. Rapp, Phys. Rev. C **71**, 034907 (2005).
[3] H. van Hees, V. Greco, and R. Rapp, Phys. Rev. C **73**, 034913 (2006).
[4] M. G. Mustafa, Phys. Rev. C **72**, 014905 (2005).
[5] F. Prino and R. Rapp, J. Phys. G **43**, 093002 (2016).
[6] Y. Xu *et al.*, Phys. Rev. C **99**, 014902 (2019).
[7] R. Rapp *et al.*, Nucl. Phys. **A979**, 21 (2018).
[8] S. Cao *et al.*, Phys. Rev. C **99**, 054907 (2019).
[9] X. Dong and V. Greco, Prog. Part. Nucl. Phys. **104**, 97 (2019).
[10] M. He, H. van Hees, and R. Rapp, Prog. Part. Nucl. Phys. **130**, 104020 (2023).
[11] J. Casalderrey-Solana and D. Teaney, Phys. Rev. D **74**, 085012 (2006).
[12] N. Brambilla, V. Leino, P. Petreczky, and A. Vairo, Phys. Rev. D **102**, 074503 (2020).
[13] L. Altenkort, A. M. Eller, O. Kaczmarek, L. Mazur, G. D. Moore, and H.-T. Shu, Phys. Rev. D **103**, 014511 (2021).
[14] N. Brambilla, V. Leino, J. Mayer-Steudte, and P. Petreczky (TUMQCD Collaboration), Phys. Rev. D **107**, 054508 (2023).
[15] L. Altenkort, O. Kaczmarek, R. Larsen, S. Mukherjee, P. Petreczky, H.-T. Shu, and S. Stendebach (HotQCD Collaboration), Phys. Rev. Lett. **130**, 231902 (2023).
[16] L. Altenkort, D. De la Cruz, O. Kaczmarek, R. Larsen, G. D. Moore, S. Mukherjee, P. Petreczky, H.-T. Shu, and S. Stendebach (HotQCD Collaboration), Phys. Rev. Lett. **132**, 051902 (2024).
[17] D. Bollweg, J. L. Dasilva Golán, O. Kaczmarek, R. N. Larsen, G. D. Moore, S. Mukherjee, P. Petreczky, H.-T. Shu, S. Stendebach, and J. H. Weber (HotQCD Collaboration), J. High Energy Phys. 09 (2025) 180.
[18] S. Caron-Huot and G. D. Moore, Phys. Rev. Lett. **100**, 052301 (2008).
[19] S. Caron-Huot and G. D. Moore, J. High Energy Phys. 02 (2008) 081.
[20] Y. Burnier, M. Laine, J. Langelage, and L. Mether, J. High Energy Phys. 08 (2010) 094.
[21] B. Scheihing-Hitschfeld and X. Yao, Phys. Rev. D **108**, 054024 (2023); B. Scheihing-Hitschfeld and X. Yao, Phys. Rev. D **109**, 099902(E) (2024).
[22] D. De la Cruz, A. M. Eller, and G. D. Moore, Phys. Rev. D **110**, 094057 (2024).
[23] C. P. Herzog, A. Karch, P. Kovtun, C. Kozcaz, and L. G. Yaffe, J. High Energy Phys. 07 (2006) 013.
[24] S. S. Gubser, Phys. Rev. D **74**, 126005 (2006).
[25] S. S. Gubser, Nucl. Phys. **B790**, 175 (2008).
[26] J. Casalderrey-Solana and D. Teaney, J. High Energy Phys. 04 (2007) 039.
[27] A. Peshier, Nucl. Phys. **A888**, 7 (2012).
[28] S. K. Das, F. Scardina, S. Plumari, and V. Greco, Phys. Rev. C **90**, 044901 (2014).
[29] F. Scardina, S. K. Das, V. Minissale, S. Plumari, and V. Greco, Phys. Rev. C **96**, 044905 (2017).
[30] A. Beraudo, J. F. Du Plessis, D. Pablos, and K. Rajagopal, J. High Energy Phys. 06 (2026) 220.
[31] K. Rajagopal, B. Scheihing-Hitschfeld, and U. A. Wiedemann, Phys. Rev. Lett. **135**, 242301 (2025).
[32] K. Rajagopal, B. Scheihing-Hitschfeld, and U. A. Wiedemann, J. High Energy Phys. 07 (2025) 013.
[33] H. Georgi, Phys. Lett. B **240**, 447 (1990).
[34] L. V. Keldysh, Sov. Phys. JETP **20**, 1018 (1965).
[35] J. S. Schwinger, J. Math. Phys. (N. Y.) **2**, 407 (1961).
[36] M. Laine and A. Vuorinen, Basics of Thermal Field Theory, Lecture Notes in Physics, Vol. **925** (Springer, Cham, 2016), 10.1007/978-3-319-31933-9.
[37] J. Ghiglieri, A. Kurkela, M. Strickland, and A. Vuorinen, Phys. Rep. **880**, 1 (2020).
[38] E. Braaten and R. D. Pisarski, Nucl. Phys. **B337**, 569 (1990).
[39] E. Braaten and R. D. Pisarski, Nucl. Phys. **B339**, 310 (1990).
[40] E. Braaten and R. D. Pisarski, Phys. Rev. D **45**, R1827 (1992).
[41] S. Caron-Huot, J. High Energy Phys. 04 (2009) 004.

[42] We denote the number of "colors" of the SU(N_c) gauge group by N_c, the number of real adjoint scalars in the theory by N_X, and the number of Dirac fermions in representation F by N_f. T_F is the index of the representation $\mathrm{Tr}[T_F^a T_F^b] = T_F \delta^{ab}$.

[43] By construction, $\mathcal{I}_{\mathrm{Match}}$ is the leading term in the expansion of $\mathcal{I}_{\mathrm{Soft}}$ in powers of $m_D^2/|\mathbf{p}|^2$, since the HTL-resummed propagator depends on the coupling and temperature only through m_D^2. Because $\mathcal{I}_{\mathrm{Match}} \propto m_D^2/|\mathbf{p}|^4$, the difference (8) follows as written.

[44] E. Braaten and M. H. Thoma, Phys. Rev. D **44**, 1298 (1991).

[45] E. Braaten and M. H. Thoma, Phys. Rev. D **44**, R2625 (1991).

[46] It is also reassuring to note that the longitudinal part of the HTL-resummed contributions (in the first two lines) in the kernel (10) satisfies the Einstein relation. This is mandated by the fact that in the extreme weakly coupled limit equilibration should still be attained, and the fact that this part of the kernel is quadratic means that the associated stochastic process is Gaussian.

[47] See Supplemental Material at http://link.aps.org/supplemental/10.1103/7fd5-1kq5 for derivations of the fixed-order soft contribution, the zero-velocity cumulants, and matching-scale invariance.

[48] J. F. Du Plessis and B. Scheihing-Hitschfeld, arXiv:2610.03863.

[49] We note that our calculation is based on the QCD Wilson line $\mathrm{P}\exp\left(ig\int A_\mu dx^\mu\right)$. A different calculation in $\mathcal{N}=4$ SYM would involve Wilson lines that also include a direct coupling of the HQ to adjoint scalars, like earlier studies of HQ diffusion in this theory have done [19,50]. However, as discussed in [32], the distinction between the two types of Wilson lines is inconsequential for the calculation of the Wilson loop (2) at strong coupling [51–53], which is what we aim to compare against here.

[50] P. M. Chesler and A. Vuorinen, J. High Energy Phys. 11 (2006) 037.

[51] L. F. Alday and J. Maldacena, J. High Energy Phys. 11 (2007) 068.

[52] J. Polchinski and J. Sully, J. High Energy Phys. 10 (2011) 059.

[53] J. Casalderrey-Solana, H. Liu, D. Mateos, K. Rajagopal, and U. A. Wiedemann, *Gauge/String Duality, Hot QCD and Heavy Ion Collisions* (Cambridge University Press, Cambridge, England, 2014), 10.1017/CBO9781139136747.

[54] ALICE Collaboration, Letter of intent for ALICE 3: A next-generation heavy-ion experiment at the LHC (2022), arXiv:2211.02491.

[55] K. Rajagopal, B. Scheihing-Hitschfeld, and U. A. Wiedemann, arXiv:2606.02693.

End Matter

Integrands—From perturbative finite temperature field theory one obtains

$$\begin{aligned}\mathcal{I}_{\mathrm{Hard}} = {}& \frac{N_c}{2}\int_{k_0}\frac{e^{\mathbf{p}\cdot\mathbf{v}/T}-1}{|e^{k_0/T}-1||e^{(\mathbf{p}\cdot\mathbf{v}-k_0)/T}-1|}\frac{\Theta(1-u^2)}{4|\mathbf{p}|}\left(\frac{(1-\mathbf{v}^2)^2\left|\mathrm{sgn}(k_0)-u\frac{\mathbf{v}\cdot\mathbf{p}}{|\mathbf{p}|}\right|}{k_0^2\left[\left(\mathrm{sgn}(k_0)-u\frac{\mathbf{v}\cdot\mathbf{p}}{|\mathbf{p}|}\right)^2-(1-u^2)\left(\mathbf{v}^2-\frac{(\mathbf{v}\cdot\mathbf{p})^2}{\mathbf{p}^2}\right)\right]^{3/2}}\right.\\ & -\frac{4(1-\mathbf{v}^2)}{\mathbf{p}^2-(\mathbf{p}\cdot\mathbf{v})^2}+\frac{8+4N_X}{[\mathbf{p}^2-(\mathbf{p}\cdot\mathbf{v})^2]^2}\left[\left(k_0-|k_0|\frac{\mathbf{p}\cdot\mathbf{v}}{|\mathbf{p}|}u\right)^2+\frac{k_0^2}{2}\left(\mathbf{v}^2-\frac{(\mathbf{p}\cdot\mathbf{v})^2}{\mathbf{p}^2}\right)(1-u^2)\right]\Bigg)\\ & -2N_fT_F\int_{k_0}\frac{e^{k_0/T}(1-e^{-\mathbf{p}\cdot\mathbf{v}/T})}{(e^{k_0/T}+1)(e^{(k_0-\mathbf{p}\cdot\mathbf{v})/T}+1)}\frac{\Theta(1-u^2)}{4|\mathbf{p}|}\left(\frac{1-\mathbf{v}^2}{\mathbf{p}^2-(\mathbf{p}\cdot\mathbf{v})^2}-\frac{4}{[\mathbf{p}^2-(\mathbf{p}\cdot\mathbf{v})^2]^2}\right.\\ & \left.\times\left[\left(k_0-|k_0|\frac{\mathbf{p}\cdot\mathbf{v}}{|\mathbf{p}|}u\right)^2+\frac{k_0^2}{2}\left(\mathbf{v}^2-\frac{(\mathbf{p}\cdot\mathbf{v})^2}{\mathbf{p}^2}\right)(1-u^2)\right]\right),\end{aligned}\tag{A1}$$

where we have introduced u as

$$u=\frac{\mathbf{p}^2+2(\mathbf{p}\cdot\mathbf{v})k_0-(\mathbf{p}\cdot\mathbf{v})^2}{2|\mathbf{p}||k_0|},\tag{A2}$$

describing the cosine of the angle between a loop momentum and $\mathbf{p}$. The Heaviside step function implies that $|\mathbf{p}|-|\mathbf{p}\cdot\mathbf{v}|<2|k_0|<|\mathbf{p}|+|\mathbf{p}\cdot\mathbf{v}|$, which in turn implies that $\mathcal{I}_{\mathrm{Hard}}$ is exponentially suppressed at large $\mathbf{p}$. Note that, at this order in Feynman gauge perturbation theory, only the two classes of perturbative diagrams shown in Fig. 2 contribute. All other topologies are either $\mathbf{L}$-independent, sub-extensive in the late-time limit, or vanish identically. In other gauges, a 3-gluon vertex diagram is also present. The result is obtained by a tedious but straightforward evaluation of integrals over delta functions; further details will be presented in Ref. [48].

Using the standard HTL-resummed gluon self-energy in the single exchange propagator [36,38,41] gives

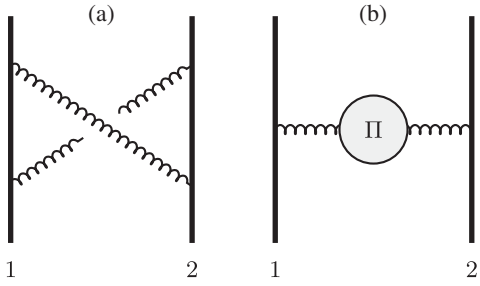


FIG. 2. Contributing order-g^4 perturbative topologies in Feynman gauge. Panel (a) denotes the crossed one-gluon exchanges between opposite contour branches; panel (b) denotes the self-energy correction to a single exchanged gluon, including gauge, fermion, and scalar contributions.

$$\mathcal{I}_{\rm Soft} = \frac{2\Gamma_E((\mathbf{p}\cdot\mathbf{v})/|\mathbf{p}|)}{\Sigma_E^2(p_0=\mathbf{p}\cdot\mathbf{v},p)+\Gamma_E^2((\mathbf{p}\cdot\mathbf{v})/|\mathbf{p}|)} + \frac{2\mathbf{v}^2\left(1-\frac{(\mathbf{p}\cdot\mathbf{v})^2}{\mathbf{p}^2\mathbf{v}^2}\right)\Gamma_T((\mathbf{p}\cdot\mathbf{v})/|\mathbf{p}|)}{\Sigma_T^2(p_0=\mathbf{p}\cdot\mathbf{v},p)+\Gamma_T^2((\mathbf{p}\cdot\mathbf{v})/|\mathbf{p}|)}. \tag{A3}$$

Expanding to lowest order in the coupling yields the contribution that has been overcounted by adding the hard and soft contributions to each other and must therefore be subtracted

$$\mathcal{I}_{\rm Match} = \frac{2\Gamma_E((\mathbf{p}\cdot\mathbf{v})/|\mathbf{p}|)}{|\mathbf{p}|^4} + \frac{2\mathbf{v}^2\left(1-\frac{(\mathbf{p}\cdot\mathbf{v})^2}{\mathbf{p}^2\mathbf{v}^2}\right)\Gamma_T((\mathbf{p}\cdot\mathbf{v})/|\mathbf{p}|)}{|\mathbf{p}|^4\left(1-\frac{(\mathbf{p}\cdot\mathbf{v})^2}{\mathbf{p}^2}\right)^2}, \tag{A4}$$

where

$$\Sigma_T(k_0=k\eta,k) = k^2(1-\eta^2) + \frac{m_D^2}{2}\left[\eta^2+\frac{\eta(1-\eta^2)}{2}\ln\left|\frac{1+\eta}{1-\eta}\right|\right], \tag{A5}$$

$$\Sigma_E(k_0=k\eta,k) = k^2 + m_D^2\left[1-\frac{\eta}{2}\ln\left|\frac{1+\eta}{1-\eta}\right|\right], \tag{A6}$$

$$\Gamma_T(\eta) = \frac{\pi m_D^2}{4}\eta(1-\eta^2), \tag{A7}$$

$$\Gamma_E(\eta) = \frac{\pi m_D^2}{2}\eta. \tag{A8}$$

Invariance under change in separation scale—Choosing an arbitrary matching scale $\Lambda \sim g^0 T$ leads to Eq. (10) changing in two simple ways: (1) the explicit logarithm in the first line $\ln(m_D/T)$ becomes $\ln(m_D/\Lambda)$, and (2) the Heaviside step function in the last line $\theta(T-|\mathbf{p}|)$ becomes $\theta(\Lambda-|\mathbf{p}|)$.

Then, differentiating with respect to Λ gives a $1/\Lambda$ for the first and a $\delta(\Lambda-|\mathbf{p}|)$ for the second. Using the explicit form of $\mathcal{I}_{\rm Match}$ (A4), it is then straightforward to check that the two contributions exactly cancel. Physically, this is because the log-enhanced contributions coming from the HTL-resummed propagator can be equivalently obtained by integrating the unresummed HTL propagator from $|\mathbf{p}| \sim m_D$ to $|\mathbf{p}| \sim g^0 T$ as discussed in [1].

Closed form of cumulants at $v=0$—From Eqs. (10) and (14) it is clear that $\mathfrak{M}_n$ for $n \geq 4$ is fully determined by the hard contribution. Introducing $k \equiv 2|k_0|/p \geq 1$, exploiting the symmetries of the integrands, it is straightforward to show that

$$K_{\rm hard}(x,0) = -\frac{g^4 C_F}{64\pi^3 T}\int_0^\infty dp\int_{-1}^1 d\mu\,\sinh^2\left(\frac{p\mu x}{2}\right)\int_1^\infty dk\left\{\frac{N_c[2k^{-2}-2+(1+N_X/2)k^2]}{\sinh^2\left(\frac{pk}{4T}\right)}+\frac{2T_F N_f(k^2-1)}{\cosh^2\left(\frac{pk}{4T}\right)}\right\}. \tag{C1}$$

Because the cumulants are given by derivatives of K as $\mathfrak{M}_n = -\partial^n K/\partial x^n|_{x=0}$, and the only scale in the problem is T, all that is needed is to evaluate the integrals

$$\tilde{\mathcal{J}}_{n,m}^{(\sinh)} \equiv \int_0^\infty dp\int_1^\infty dk\frac{p^n k^m}{\sinh^2\left(\frac{pk}{4}\right)} = \frac{2^{n+3}n!\zeta(n)}{(n-m)}, \tag{C2}$$

$$\tilde{\mathcal{J}}_{n,m}^{(\cosh)} \equiv \int_0^\infty dp\int_1^\infty dk\frac{p^n k^m}{\cosh^2\left(\frac{pk}{4}\right)} = (1-2^{1-n})\tilde{\mathcal{J}}_{n,m}^{(\sinh)}. \tag{C3}$$

Using these to evaluate the cumulants yields

$$\mathfrak{M}_n(0) = \frac{3g^2 C_F m_D^2 2^{n-1} T^{n-2}(n-1)!\zeta(n)}{\pi^3(n+1)\left(N_c + \frac{N_c N_X}{2} + T_F N_f\right)} \left[\frac{N_c(N_X n(n+2) + 2(n^2-2n+8))}{8(n-2)(n+2)} + \frac{(1-2^{1-n})T_F N_f}{n-2}\right] \tag{C4}$$

for all even $n \geq 4$, while $\mathfrak{M}_n(0) = 0$ for odd n. The explicit $(n-2)^{-1}$ pole signals the special infrared sensitivity of the diffusion coefficient, and is precisely why the $n = 2$ case must be treated separately.

HQ diffusion coefficient at $v = 0$—The heavy quark momentum diffusion coefficient is determined in terms of $\mathfrak{M}_2(0)$ as

$$\kappa \equiv T\mathfrak{M}_2(0). \tag{D1}$$

We set $N_X = 0$ for easier comparison with the QCD literature. To evaluate $\mathfrak{M}_2(0)$, it is convenient to analytically continue the hard result in Eq. (C4) in n, combine it with the quadratic HTL-matching part of Eq. (10) also analytically continued in n, and then take the limit $n \to 2$. The poles cancel in the sum, as they must. We obtain

$$\kappa = \frac{g^2 C_F m_D^2 T}{6\pi}\left[\ln\left(\frac{2T}{m_D}\right) + \frac{T_F N_f \ln 2}{N_c + T_F N_f} + \xi\right] \tag{D2}$$

with $\xi = \frac{1}{2} - \gamma_E + (\zeta'(2)/\zeta(2))$, in agreement with the known leading-order heavy quark diffusion coefficient [1,20].

$R(v)$ in the ultra-relativistic limit at weak coupling. In the $v \to 1$ limit the dominant contribution to the large-n cumulants comes from nearly collinear corners of the hard integrand, where $\mathbf{p}\cdot\mathbf{v} \simeq |\mathbf{p}|$, asymptotically pinched against the kinematic boundary imposed by $\Theta(1-u^2)$, which sets the boundaries of the k_0 integral to be $k_0 > (|\mathbf{p}| + \mathbf{p}\cdot\mathbf{v})/2$ and $k_0 < -(|\mathbf{p}| - \mathbf{p}\cdot\mathbf{v})/2$. To isolate these corners it is convenient to introduce

$$\ell \equiv \frac{k_0}{p}, \qquad q \equiv (1-v^2)\frac{p}{T}. \tag{D3}$$

The variable ℓ makes the kinematic support asymptotically independent of p, since the hard-region bounds are linear in p, while q removes the leading velocity dependence of the singularity driven by the difference between $\mathbf{p}\cdot\mathbf{v}$ and $|\mathbf{p}|$. Since $p = \gamma^2 T q$, the n th moment weight contributes a factor $(\gamma^2 T)^n$, which is the origin of the $\gamma^{2n}T^n$ scaling quoted in the main text. Schematically, the remaining q-integral produces the factorial growth through $\int dq\, q^n/(e^q - 1) = n!\zeta(n+1)$. A more detailed account will be given in [48]. The conclusion of this analysis is that as $\gamma \to \infty$ one has

$$R(v) \sim 1/(4\gamma^2 T). \tag{D4}$$

$R(v)$ in the ultra-relativistic limit at strong coupling—In light of the Legendre transform map $x = \partial\tilde{S}/\partial C_L$, and because the explicit expression for $\tilde{S}$ is known [32], the radius of convergence of $K(x)$ in strongly coupled $\mathcal{N} = 4$ SYM can be determined by directly calculating the derivative of $\tilde{S}$ with respect to C_L at large $|C_L|$ (considering both positive and negative C_L separately). Going through this calculation, to be discussed in more detail in [48,55], one finds

$$r_0 = \frac{8\sqrt{2}\Gamma(7/4)^2}{3\sqrt{\pi}} \approx 1.7972. \tag{D5}$$